Mechanical Transients Initiated by Photolysis of Caged ATP within Fibers of Insect Fibrillar Flight Muscle

M. YAMAKAWA and Y. E. GOLDMAN

From the Department of Physiology and Pennsylvania Muscle Institute, University of Pennsylvania, School of Medicine, Philadelphia, Pennsylvania 19104

ABSTRACT Kinetics of the cross-bridge cycle in insect fibrillar flight muscle have been measured using laser pulse photolysis of caged ATP and caged inorganic phosphate (P_i) to produce rapid step increases in the concentration of ATP and P_i within single glycerol-extracted fibers. Rapid photochemical liberation of 100 μM–1 mM ATP from caged ATP within a fiber caused relaxation in the absence of Ca^{2+} and initiated an active contraction in the presence of ~30 μM Ca^{2+}. The apparent second order rate constant for detachment of rigor cross-bridges by ATP was between 5×10^4 and 2×10^5 $M^{-1}s^{-1}$. This rate is not appreciably sensitive to the Ca^{2+} or P_i concentrations or to rigor tension level. The value is within an order of magnitude of the analogous reaction rate constant measured with isolated actin and insect myosin subfragment-1 (1986. *J. Muscle Res. Cell Motil.* 7:179–192). In both the absence and presence of Ca^{2+} insect fibers showed evidence of transient cross-bridge reattachment after ATP-induced detachment from rigor, as found in corresponding experiments on rabbit psoas fibers. However, in contrast to results with rabbit fibers, tension traces of insect fibers starting at different rigor tensions did not converge to a common time course until late in the transients. This result suggests that the proportion of myosin cross-bridges that can reattach into force-generating states depends on stress or strain in the filament lattice. A steady 10-mM concentration of P_i markedly decreased the transient reattachment phase after caged ATP photolysis. P_i also decreased the amplitude of stretch activation after step stretches applied in the presence of Ca^{2+} and ATP. Photolysis of caged P_i during stretch activation abruptly terminated the development of tension. These results are consistent with a linkage between P_i release and the steps leading to force production in the cross-bridge cycle.

INTRODUCTION

Insect fibrillar flight muscle has several characteristics that contribute to its importance in studies of the mechanism of contraction. First, its filament lattice is well

Address reprint requests to Dr. Yale E. Goldman, Department of Physiology, University of Pennsylvania, School of Medicine, D701 Richards Building, Philadelphia, PA 19104-6085.

Dr. Yamakawa's present address is Bockus Research Institute, The Graduate Hospital, One Graduate Plaza, Philadelphia, PA 19146.

J. GEN. PHYSIOL. © The Rockefeller University Press · 0022-1295/91/10/0657/23 $2.00
Volume 98 October 1991 657–679

ordered, allowing some of the earliest (Reedy, Holmes, and Tregear, 1965; Ashhurst, 1967) and most detailed (Taylor, Reedy, Córdova, and Reedy, 1989) information to be obtained on the structure of cross-bridges between the thick and thin filaments. Second, stretch activation (Pringle, 1978) is most highly developed in these muscles. When the myofibrils are immersed in an activating solution containing Ca^{2+} and adenosine triphosphate (ATP), the full contraction develops only several hundred milliseconds after application of a small mechanical stretch. Other muscles, notably heart muscle, show an analogous delayed tension rise after stretch (Steiger, 1971; Bozler, 1972), indicating that this is a basic property of the contractile mechanism. However, stretch activation is more prominent in insect flight muscle. In concert with the resonant system of the cuticle and load of the wings, stretch activation is the mechanical property of the muscle that produces the wing beating oscillatory contractions in vivo. The characteristic delayed tension rise after stretch is found in muscle fibers with chemically disrupted surface membranes, implying that stretch activation is an intrinsic property of the myofibrillar contractile mechanism (Jewell and Rüegg, 1966).

Two main hypotheses are currently considered as possible mechanisms for triggering stretch activation. The helical periodicities of the thick and thin filaments have identical axial spacing (38.7 nm), so the number of myosin heads aligned with thin filament target sites, appropriately oriented for attachment, may become maximal every 38.7 nm of filament sliding. Stretch of the muscle in activating solution may bring myosin heads into register with the attachment sites and thereby lead to development of fully active tension (Wray, 1979; Abbott and Cage, 1984). Alternatively, stretching a muscle in activating solution may alter the kinetic parameters of the cross-bridge cycle via a stress or strain sensor. Either an increased attachment rate (Thorson and White, 1969) or a decreased detachment rate (Pringle, 1978; Thorson and White, 1983; Güth, Poole, Maughan, and Kuhn, 1987) of cycling cross-bridges would enhance the proportion of cross-bridges attached and the force. This postulated alteration in kinetics might be controlled by strain in elastic connections (C filaments, possibly mini-titin; Nave and Weber, 1990) between the thick filaments and the Z-line in insect flight muscle (Auber and Couteaux, 1963; White and Thorson, 1973; White, 1983) or via an unusual structure such as troponin-H that might serve as a length or strain sensor (Bullard, Leonard, Larkins, Butcher, Karlik, and Fyrberg, 1988).

Rates of several of the cross-bridge reaction steps have been measured in vertebrate skeletal muscle using a photochemical technique to abruptly initiate the cross-bridge cycle from rigor (Goldman, Hibberd, McCray, and Trentham, 1982; Goldman, Hibberd, and Trentham, 1984*a*, *b*; Hibberd, Dantzig, Trentham, and Goldman, 1985). A photolabile precursor, caged ATP (Kaplan, Forbush, and Hoffman, 1978), is allowed to diffuse into the filament lattice of single fibers in rigor. Laser pulse photolysis then liberates ATP that binds to the cross-bridges, leading to detachment and further reactions of the cross-bridge cycle.

In this work we have used the laser photolysis technique to study insect fibrillar flight muscle. In particular, we studied the effects of mechanical strain on rates of cross-bridge detachment and subsequent reattachment to test the various hypotheses for stretch activation.

Some of the experiments have been reported in preliminary form (Yamakawa, Güth, Hibberd, and Goldman, 1985).

METHODS

Fiber Preparations

Lethocerus indicus were collected by Dr. S. Ratanabhuma (Chiang Mai University, Thailand) and *Lethocerus collosicus* by Mrs. Aneta (Sister Sam) and Claudius Samuels, private collectors, in Black River, Jamaica. Muscle and other tissues overlying the dorsal longitudinal flight muscles (DLM) were quickly removed, and the DLM attached to the thorax were placed in an extraction solution at 4°C containing 100 mM KCl, 5 mM EGTA, 3.5 mM KH_2PO_4, 5.5 mM K_2HPO_4, 1 mM NaN_3, 0.25 mM $MgCl_2$, and 2 mM reduced glutathione, pH 6.8, mixed 1:1 with glycerol. After 5 min, the bundles were transferred to fresh extraction solution at 4°C, which was stirred gently and changed at least twice more during the next 24 h. The muscles were then transferred to fresh extraction solution and stored at −22°C for 2 wk–8 mo until used. Stretch activation was tested in each experimental preparation and was well maintained during the storage period.

Single fibers from the glycerol-extracted bundles were dissected under silicone oil at 10°C and trimmed to 2.5–4 mm in length. To obtain a firm attachment at each end, a ~0.5-mm length of fiber was coated with glue made from nitrocellulose dissolved in acetone. The layer of glue, 10–20 μm thick, hardened in 20–60 s. The fiber was submerged in the silicone oil during this period to avoid exposure to air. The reinforced ends of the fibers were clamped in T-shaped aluminum foil clips made by photolithography (Goldman and Simmons, 1984). The T-clips were then attached to steel hooks on a tension transducer and length driver.

In comparison to attaching clips directly to the myofibrils as is done with vertebrate muscles, the extra procedure of coating the ends of insect fibers with glue markedly decreased a tendency of fibers to break during transfer between different solutions in rigor photolysis trials. The coating also improved the uniformity of sarcomere length near the clamped ends. The glue did not cause any other appreciable changes in mechanical performance.

To test the effects of glycerol extraction and storage, in some experiments DLM were dissected and promptly skinned mechanically without glycerol extraction. In this case the fibers were split longitudinally using tungsten needles to disrupt the surface membrane diffusion barrier.

Apparatus

The laser photolysis technique and associated instrumentation used in this study were essentially the same as described by Goldman et al. (1984*a*) for experiments on rabbit muscle fibers. Briefly, skinned fibers were mounted horizontally in a 20- or 60-μl trough between an oil-damped semiconductor strain gauge (AE801, natural frequency 5 kHz, Akers; Goldman and Simmons, 1984) and a ceramic piezoelectric stack used to apply length changes. The solutions bathing the fiber were exchanged by a microprocessor-based controller that lowered the trough assembly, moved a different trough under the fiber, and then raised the trough assembly again. The fiber was held in place during this procedure.

Muscle fibers were put into rigor in the absence of ATP, and then caged ATP was allowed to diffuse into the filament lattice. A 50-ns, 20–150-mJ pulse of 347 nm radiation from a frequency-doubled ruby laser photolyzed caged ATP in the trough through a fused silica window. 0.1–1.2 mM ATP was liberated within the filament lattice by photolysis. The ATP initiated cross-bridge detachment and subsequent reactions which were monitored by measuring fiber tension and stiffness. The signals were recorded on a strip chart recorder, storage oscilloscope, and computer diskettes as previously described (Goldman et al., 1984*a*).

The piezoelectric stack was used to impose a continuous 1-μm, 500-Hz sinusoidal length oscillation on the fiber for the stiffness measurements. The sinusoidal components of force were separated from the force signal by a notch filter and a lock-in amplifier (Goldman et al., 1984*a*). The reference phase for demodulating the sinusoidal tension was set for each fiber to the phase of the tension response in rigor. Thus in-phase stiffness is the amplitude of the sinusoidal tension component in phase with the rigor elasticity and is interpreted as a qualitative indication of the extent of cross-bridge attachment (Goldman et al., 1984*a*). Quadrature stiffness, proportional to the amplitude of the sinusoidal tension 90° out-of-phase with the length change, is an indication of cross-bridge viscoelasticity. Quadrature stiffness is set to zero in rigor and is positive during active contractions.

In some experiments the in-phase and quadrature stiffness signals were obscured for the first 10–50 ms by transient deflections excited by instantaneous tension changes caused by the laser pulse (e.g., initial upward deflection of the quadrature (Q) traces in Fig. 4 *B*) or by length changes (e.g., initial upward deflection in Fig. 7 *A*). These artifacts are due to leakage of frequency components in the wide spectral band of abrupt tension changes through the lock-in amplifier (Goldman et al., 1984*a*). They could easily be distinguished from valid changes of the stiffness signals because their sign was random and their fast time course was unrelated to events in the tension signal. For instance, the quadrature trace of Fig. 4 *B* shows both the artifactual (smaller) deflection, identified with an asterisk, and the actual signal (larger prolonged deflection).

Solutions

The solutions used as bathing media for the fibers are listed in Table I, except as noted in the text and figure legends. Details on preparation of the solutions are given in Goldman et al. (1984*a*). The experiments were conducted at room temperature (18–20°C) and pH 7.1. Except where noted, the total ionic strength of the solutions was 200 mM. Reagent grade ATP (vanadium-free), creatine phosphokinase, creatine phosphate, reduced glutathione, and TES pH buffer were obtained from Sigma Chemical Co. (St. Louis, MO). EGTA, $MgCl_2$, KOH, HCl, NaOH, NaN_3, KH_2PO_4, K_2HPO_4, and other components were obtained from Fisher Scientific Co. (Pittsburgh, PA).

Photochemical Compounds and Assays for Photochemical Conversion

The caged ATP used in this study was kindly supplied by Dr. D. R. Trentham (N.I.M.R., Mill Hill, London, UK). It was synthesized either by condensation of caged P_i with ADP morpholidate as previously described (Goldman et al., 1984*a*) or by condensation of 1-(2-nitrophenyl)diazoethane with ATP (Walker, Reid, McCray, and Trentham, 1988). In either case the product was purified by high-performance liquid chromatography (HPLC; Waters Associates, Milford, MA) using a reverse phase C-18 preparative column and then by anion exchange chromatography (on DEAE) to reduce the concentrations of contaminant ATP and ADP to $<0.01\%$ of the caged ATP concentration (Goldman et al. 1984*a*).

After photolysis of caged ATP, the contents of the muscle fiber trough were transferred by suction to small polypropylene vials, frozen, and stored at −22°C for subsequent assay of ATP liberation. The samples were analyzed by HPLC using an anion exchange (SAX) column and eluting solvent of 0.4 M ammonium phosphate buffer, at pH 4.3, and methanol (92:8 vol/vol). Absorption at 254 nm was monitored in the eluate, and the integral of the ATP peak above baseline was related to that produced by a 1-mM ATP standard. Samples were run at least in duplicate and for each sample the average of two or more runs was taken as the final ATP concentration liberated from caged ATP.

Caged P_i was prepared as described by Dantzig, J. A., Y. E. Goldman, J. Lacktis, and E. Homsher (manuscript submitted for publication). The values given in the text for P_i liberation

were calculated from the energy (in millijoules) of the laser pulse for each trial and a calibration factor of 11.6 μM P_i released per mJ of laser energy (Dantzig, J. A., and Y. E. Goldman, personal communication) obtained using ^{32}P caged P_i kindly supplied by Dr. E. Homsher.

Experimental Protocol

A fiber with T-clips, 1.4–2.5 mm in length between the glued sections, was mounted slack in the experimental setup in relaxing solution and stretched under visual observation until the slack was taken up. The fiber was then stretched an additional 1–2% until the resting stiffness

TABLE I

A. Solutions used in the experiments in the absence of P_i

Constituents	Rel	Act	0.1 Rel	Rigor	Ca.rigor
Na_2ATP	5.4	5.5	0.1	0.0	0.0
$MgCl_2$	7.7	6.8	2.7	3.2	1.3
EGTA	25.0	0.0	30.0	52.7	0.0
CaEGTA	0.0	25.0	0.0	0.0	20.0
TES	100.0	100.0	100.0	100.0	100.0
CP	19.1	19.5	22.0	0.0	0.0
HDTA	0.0	0.0	0.0	0.0	32.6
GSH	10.0	10.0	10.0	10.0	10.0

B. Solutions used in the experiments in the presence of 10 mM P_i

Constituents	Rel	Act	Rigor	Ca.rigor
Na_2ATP	5.5	5.5	0.0	0.0
$MgCl_2$	7.8	7.2	3.3	1.5
EGTA	15.0	0.0	45.2	0.0
CaEGTA	0.0	15.0	0.0	20.0
TES	100.0	100.0	100.0	100.0
CP	23.1	23.3	0.0	0.0
HDTA	0.0	0.0	0.0	28.1
GSH	10.0	10.0	10.0	10.0

Concentrations above are in millimolar. All solutions had 200 mM ionic strength, pH 7.1 (adjusted with HCl or KOH) at room temperature (20°C) and 1 mM free Mg^{2+}. In Rel, 0.1 Rel, and Act solutions, [MgATP] was 5.0 mM. In Rel, 0.1 Rel, and Rigor solutions, free $[Ca^{2+}]$ was $< 10^{-8}$ M. In Act and Ca.rigor, free $[Ca^{2+}]$ was ~30 μM. Solutions with CP had 1 mg/ml creatine phosphokinase added.

EGTA, ethyleneglycol-*bis*-(β-aminoethylether)-*N,N,N',N'*-tetraacetic acid.

TES, *N*-tris(hydroxymethyl)methyl-2-aminoethanesulphonic acid.

CP, creatine phosphate.

HDTA, 1,6-diaminohexane-*N,N,N',N'*-tetraacetic acid.

GSH, reduced glutathione.

reached ~1 μN/μm for a typical 2-mm fiber. The fiber was washed twice in relaxing solution (5 mM MgATP) and visually inspected for damage. Fiber length, sarcomere length, and cross-sectional area were measured using a compound microscope as described in Goldman and Simmons (1984).

At the beginning of each experiment the fiber was transferred to the activating solution, and a 0.5–1% quick stretch was applied to test stretch activation. The fiber was placed again in 5 mM MgATP relaxing solution for 5 min or more, and a corresponding baseline was recorded with an equivalent stretch. If the ratio of the peak amplitude of delayed tension increase during

stretch activation to that of the passive tension increase was <0.5, stretch activation was considered to be insufficient and a new fiber was selected.

The fiber was equilibrated with 0.1 mM MgATP relaxing solution (0.1 Rel, Table I) and then put into Ca^{2+}-free rigor. For photolysis trials in the absence of Ca^{2+}, the fiber went through two further washes in rigor solution and then rigor solution with 10 mM added caged ATP. In the trials with Ca^{2+} present, the fiber was put into Ca^{2+}-free rigor solution, then equilibrated with 30 μM free Ca^{2+} (Ca-rigor solution) and Ca-rigor with 10 mM added caged ATP. In some cases caged ATP solutions also contained 10 mM P_i (Table I).

2 min or more were allowed for caged ATP to diffuse into the fiber, and then the laser was triggered to liberate ATP. The fiber was then relaxed in 0.1 mM ATP relaxing solution. Four to six photolysis trials of this type were performed on each fiber. The fiber was then put into 5 mM ATP relaxing solution for at least 5 min, and finally the level of stretch activation was tested again in activating solution.

Preliminary experiments showed that in some fibers, more than six repeated photolysis trials on the same fiber caused a decrease in sensitivity to ATP. The data presented in this paper were taken from the first two to four photolysis trials in most cases and from up to six trials if the fiber maintained a substantial stretch activation through the end of the experiment. Stretch activation was often well maintained after four to six photolysis trials.

RESULTS

Maintenance of Stretch Activation

In initial experiments stretch activation was markedly suppressed after several cycles of rigor contraction, addition of caged ATP, and relaxation by photolysis (Yamakawa et al., 1985). Since stretch activation is the mechanical characteristic that leads to the physiological oscillatory contractions, we further investigated the relationship between the photolysis procedure and maintenance of stretch activation. Fig. 1 *A* shows tension traces from a single glycerol-extracted insect flight muscle fiber after quick stretches of 0.9% fiber length. The trace labeled *act 1* was recorded in activating solution at the beginning of an experiment and trace *rel* was the response to the same stretch in relaxing solution.

In activating solution, tension (*1*) increased concurrently with the length trace, (*2*) fell during the next few milliseconds, (*3*) increased again for the next 100–200 ms, and (*4*) finally fell to an intermediate value during the next 0.5–1 s. Phases 1 and 2 are not well resolved at the time scale plotted in Fig. 1. The 100–200-ms delayed tension increase (phase 3) is the primary characteristic of stretch activation.

After the initial test of stretch activation, the fiber was put into rigor and relaxed by photolysis of caged ATP several times. (Fig. 1 *B*; The kinetics of relaxation by photolysis are described in the next section.) Stretch activation was then tested in activating solution and found to be markedly suppressed (trace *act 2* in Fig. 1 *A*). However, if the fiber was released by 200 μm (~15% of the fiber length), left slack in the activating solution for ~2 min, and then stretched back to the original length (termed "toggling procedure"), the steady isometric tension was increased and stretch activation was restored (*act 3*). Stretch activation was often substantially restored by this procedure after several (two to six) photolysis trials. This result indicates that the suppression of stretch activation after one to four photolysis trials we previously reported (Yamakawa et al., 1985) does not imply irreversible damage to the fiber.

After a larger number of photolysis trials (> 10), the toggling procedure did not restore stretch activation. Compared with the standard conditions (10 mM reduced glutathione, 200 mM ionic strength, pH 7.1), increasing the glutathione concentration to 40 mM or reducing ionic strength to 160 mM or pH to 6.8 did not markedly reduce the irreversible suppression. The suppression of stretch activation was probably caused by a combination of factors: mechanical disruption due to the multiple solution exchanges, exposure of the fiber to air, and reactions of the photolysis by-product, 2-nitroso-acetophenone.

Photolysis of Caged ATP in the Absence of Ca^{2+}

Fig. 2 *A* shows tension (T), in-phase stiffness (S), and 90° quadrature stiffness (Q) during photolysis of caged ATP in a rigor fiber held at fixed length in the absence of

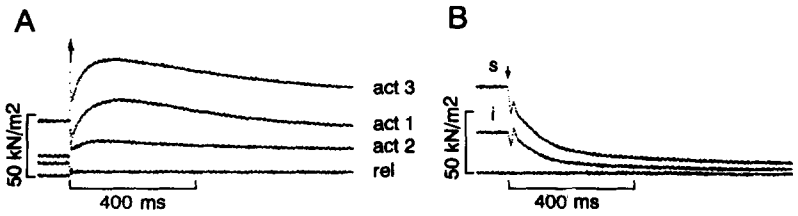

FIGURE 1. Experimental protocol to test for stretch activation during photolysis experiments. (*A*) Tension response to quick stretches of 0.89% of fiber length (*arrow*) in activating (traces labeled *act*) and relaxing (*rel*) solutions. *Act 1* was recorded at the beginning of an experiment. *Act 2* was recorded after several rigor contractions which were relaxed by photolysis of caged ATP. Stretch activation appeared to be markedly suppressed. *Act 3* was recorded after allowing the fiber to remain slack for 2 min and then restretching it back to its original length ("toggling procedure"). After the toggling, stretch activation was restored. *Act* (+Ca^{2+}, no P_i) and *rel* (0 Ca^{2+}, 0 P_i) solutions are listed in Table I. (*B*) Tension traces during relaxation from rigor after release of 0.67 mM ATP by photolysis of caged ATP (*arrow*) in the absence of Ca^{2+} and P_i. For trace *i*, the fiber was held isometric, whereas for trace *s* the fiber was stretched by 0.59% of its length 0.5 s before the laser pulse. The same fiber was used for *A* and *B*. Traces *i* and *s* were recorded between trace *act 1* and *act 2*. The lowest trace in *B* is the tension baseline recorded in the photolysis solution 2 min after the laser pulse. Fiber length, 1.40 mm; sarcomere length, 2.8 μm; cross-sectional area, 1,410 μm^2.

Ca^{2+}. The laser UV pulse was triggered at the time indicated by the arrow, and 330 μM ATP was liberated from caged ATP. The tension trace showed several phases during relaxation from rigor: an initial tension decrease lasting ~ 10 ms, an increase for the next ~ 15 ms, and finally, a slower relaxation to the baseline. For a series of eight transients after release of 500–800 μM ATP, the half-time for final tension relaxation following the peak of the tension rise was 81.2 ± 11.2 ms (mean ± SEM).

In contrast to tension, in-phase stiffness declined monotonically after the laser pulse. Two clearly resolved phases of stiffness decay were observed. The circles superimposed on the stiffness trace of Fig. 2 *A* show the sum of two exponentially decaying components fitted to the data by nonlinear least-squares regression (McCalla, 1967). The two rate constants averaged 66.3 ± 4.1 and 5.6 ± 1.1 s^{-1} (means ± SEM, $n = 8$) for the fast and slow components, respectively, at ATP

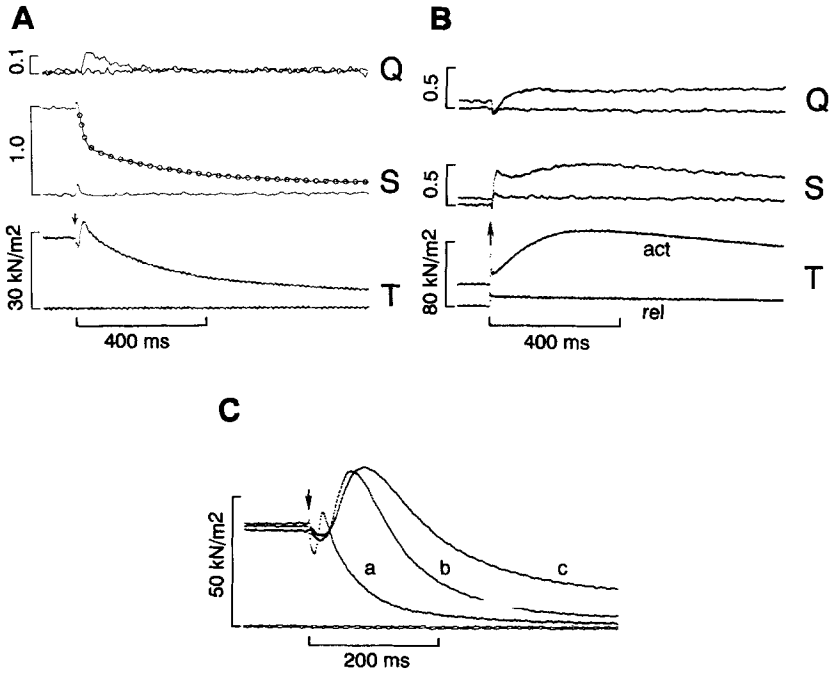

FIGURE 2. Comparison of stretch activation with the transient rise of tension after photolysis of caged ATP. (*A*) Relaxation induced by release (*arrow*) of 0.33 mM ATP from caged ATP in the absence of Ca^{2+} and P_i. *T*, tension; *S*, stiffness in-phase with a 500-Hz sinusoidal length change; *Q*, quadrature stiffness, 90° out of phase with the length oscillation. The lower flat *T*, *S*, and *Q* traces are baselines recorded in the photolysis solution 2 min after the laser pulse. The scales for *S* and *Q* are relative to in-phase rigor stiffness. The circles superimposed on the in-phase stiffness record show the fit of the sum of two exponential decay terms with the form

$$S = 0.48\, e^{-t/14} + 0.52\, e^{-t/294}$$

where *S* is the stiffness relative to rigor stiffness and *t* is the time in milliseconds after the laser pulse. Fiber length, 1.42 mm; sarcomere length, 2.6 μm; cross-sectional area, 2,630 μm^2. (*B*) Tension (*T*) and stiffness (*S* and *Q*) during stretch activation initiated (*arrow*) by a 1.0% quick stretch when the fiber was in activating solution. Lower *T*, *S*, and *Q* traces are baselines recorded during an equivalent stretch in relaxing solution. The transient deflections of the *S* and *Q* traces at the time of the length change and lasting ~50 ms are artifacts of the stiffness measurement technique. Fiber length, 1.58 mm; sarcomere length, 2.6 μm; cross-sectional area, 1,880 μm^2. (*C*) Relaxation of tension after release (*arrow*) of 0.66 mM (*a*), 0.20 mM (*b*), and 0.17 mM ATP (*c*) in the absence of Ca^{2+} and P_i. Fiber length, 2.08 mm; sarcomere length, 2.9 μm; cross-sectional area, 2,790 μm^2.

concentrations in the range of 500–800 μM. The relative amplitude of the slow component was 0.37 ± 0.06 of the total stiffness decay.

After the laser pulse, the quadrature stiffness signal increased from its zero rigor level to a peak 20–30 ms after the laser pulse and then decayed back to zero during the final phase of tension relaxation. The positive deflection of the quadrature trace indicates quick stress relaxation in the fiber similar to that present in active

contractions and after stretch activation. In-phase and quadrature stiffness both increased during stretch activation initiated by a quick stretch (Fig. 2 *B*). The time course of tension development and positive quadrature stiffness were slower than after photolysis of caged ATP.

Fig. 2 *C* shows the effect of altering the concentration of ATP liberated from caged ATP by changing the energy of the laser pulse. The final ATP concentrations measured by HPLC analysis of the trough contents were 660, 200, and 170 μM for traces *a*, *b*, and *c*, respectively. As the ATP concentration was lowered, the initial tension decrease was slower and smaller in amplitude, the tension rise was slower but larger in amplitude, and final relaxation was slowed.

These results are all qualitatively similar to those observed with rabbit psoas fibers (Goldman et al., 1984*a*). The results suggest that after caged ATP photolysis in insect flight muscle, the rigor cross-bridges detach during the initial tension decline, reattach into actively force-generating states during the tension rise, and detach again during final relaxation.

To test whether strain on the rigor cross-bridges alters the detachment kinetics, small stretches or releases were applied to the muscle fibers in rigor 0.5 or 1 s before triggering the photolysis laser pulse. Figs. 1 *B* and 3, *A* and *B*, show tension records from experiments in which isometric (traces labeled *i*), pre-stretch (*s*), and/or pre-release (*r*) trials were compared. Stretching the muscle fiber before liberation of ATP increased the rate and amplitude of the initial tension drop, but had only minor effects on the timing of the following tension rise and final relaxation. When a release was applied before the laser pulse, the initial tension decrease was suppressed or absent and the subsequent tension rise often resulted in force production above the level of rigor tension. The time of peak tension tended to be slightly (0–8 ms) later for stretches and earlier for releases, than in isometric trials (e.g., Fig. 5 *A*). Tension traces from isometric, pre-stretch, and pre-release trials did not converge and meet until relaxation was nearly complete, 0.2–1 s after the laser pulse. This result contrasts markedly with the corresponding experiments in rabbit psoas muscle (Goldman et al., 1984*a*), where the tension traces from pre-stretch, pre-release, and isometric recordings all converged 10–20 ms after the laser pulse and final relaxation proceeded with a common time course. An example of this behavior in transients recorded from a rabbit fiber is shown in Fig. 3 *C* for comparison.

The slow convergence of the tension traces in insect fibers is not due to their high resting stiffness, because the tension increment due to a stretch in relaxing solution is much smaller than the difference after photolysis between traces in isometric and pre-stretch or pre-release trials. The lowest trace in Fig. 1 *A* shows the tension increment during a 0.89% stretch in relaxation to compare with the effect of a 0.59% stretch applied before the *s* trace in Fig. 1 *B*.

In experiments with rabbit fibers, it was useful to obtain the numerical difference between two tension traces that started at different rigor tensions. Such difference traces (Fig. 3 *C*, *bottom*) show a single decay process which was interpreted as detachment of the initial rigor cross-bridges (Goldman et al., 1984*a*). Analogous difference traces for the insect muscle fibers (Fig. 3, *A* and *B*, traces $s - i$ and $i - r$) showed (*a*) a fast decay, (*b*) a plateau or reversal, and (*c*) a slower phase of decline lasting almost the full duration of tension relaxation. The phases of the difference

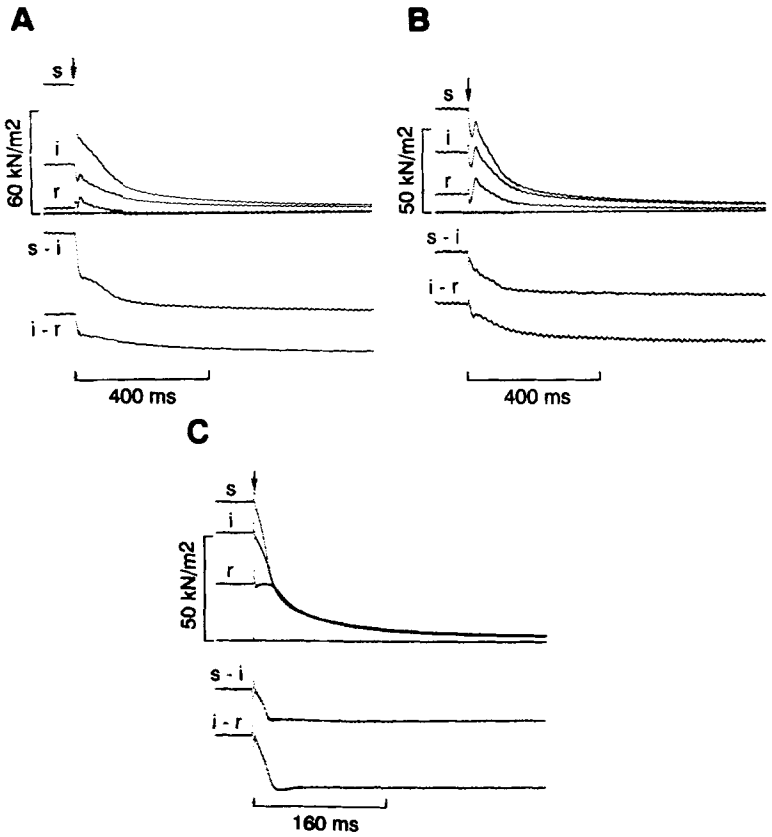

FIGURE 3. Comparison of relaxation from rigor by laser photolysis of caged ATP in the absence of Ca^{2+} and P_i in insect (*A* and *B* , in this study) and rabbit (*C*, Goldman et al., 1984*a*) muscle fibers. Traces labeled *i* were in isometric conditions. *s* indicates pre-stretches and *r* indicates pre-releases applied 0.5 s before the laser pulse. (*A*) 0.77 mM ATP released. The pre-photolysis length changes were 1.2% of fiber length. Fiber length, 1.39 mm; sarcomere length, 2.6 μm; cross-sectional area, 1,720 μm^2. (*B*) 0.66 mM ATP released. The pre-photolysis length changes were 0.43% of fiber length. Fiber length, 1.92 mm; sarcomere length, 2.9 μm; cross-sectional area, 1,750 μm^2. (*C*) Rabbit psoas muscle fiber. 0.56 mM ATP released. The pre-photolysis stretch was 0.38% and the release was 0.76% of fiber length. Fiber length, 2.18 mm; sarcomere length, 2.46 μm; cross-sectional area, 4,720 μm^2. The flat traces are tension baselines in the photolysis solution. The lowest traces ($s - i$ and $i - r$) are numerical differences between tension signals that started at different rigor force values. Note the slow decay in the insect fiber difference traces which is absent in the rabbit fiber data.

traces are correlated in time with (*a*) the initial tension decline, (*b*) tension rise and the time differential, mentioned above, between peak tensions among the individual tension traces, and (*c*) final relaxation. Phases (*b*) and (*c*) are not present in the tension difference traces from rabbit fibers that decayed to zero or became negative well before final relaxation of tension (Fig. 3 *C*).

If the decay of the difference traces simply represents detachment of the initial

rigor cross-bridges, the results would suggest that a population of cross-bridges detaches on the 100-ms time scale. Alternatively, the difference traces might contain components due to reattaching cross-bridges. In that case, the force of reattaching cross-bridges is substantially modulated by the length change before the laser pulse. This property of the transients may relate to the mechanism of stretch activation and is taken up again in the Discussion.

Photolysis of Caged ATP in the Presence of Ca^{2+}

Isometric tension traces recorded in the absence and presence of ~30 μM free Ca^{2+} (Fig. 4 *A*) superimposed during the initial tension decline and during the first part of the tension rise. But then the $+Ca^{2+}$ trace rose further and a steady component of active tension was maintained. Fig. 4 *B* shows that after photolysis of caged ATP in the presence of Ca^{2+}, in-phase stiffness (*S*) remained at a value intermediate between that of rigor and relaxation. Quadrature stiffness (*Q*) remained at a positive value. A 0.96% stretch applied to the fiber 400 ms after photolysis initiated a further, delayed tension increase (Fig. 4 *C*). This experiment shows that in the practically steady-state situation after photolysis, the condition of the fiber is similar to that in activating solution; i.e., partially activated and capable of further activation by a stretch. Compared with the rate of stretch activation, the tension rise 20–50 ms after photolysis (in either the presence or absence of Ca^{2+}) was more rapid.

Photolysis of Caged ATP in the Presence of P_i

The effects of including 10 mM inorganic phosphate (P_i) in the photolysis medium in rabbit fiber experiments suggested that the P_i release step of the cross-bridge cycle is linked to development of tension (Hibberd et al., 1985). To test the relationship of P_i release to force generation in insect muscle, photolysis experiments were performed in the presence and absence of P_i. Fig. 5 shows tension traces recorded during photolysis of caged ATP in the absence (*A* and *C*) and presence (*B* and *D*) of 10 mM P_i. Each panel shows an isometric trial (*i*), one in which the fiber was released (*r*) by 0.5%, 0.5 s before the laser pulse, and the numerical difference between the two ($i - r$).

In the absence of Ca^{2+} (*A* and *B*), addition of a steady 10-mM concentration of P_i led to a decrease in amplitude of the transient tension rise after caged ATP photolysis, convergence of the traces starting at different rigor tensions, and an acceleration of the final relaxation phase. P_i reduced or eliminated the slow phase of decay in the tension difference traces (Fig. 5 *B*, lowest trace).

In the presence of 30 μM free Ca^{2+} and zero P_i (Fig. 5 *C*) traces beginning at different rigor tensions did not reach the same steady tension after ATP liberation; i.e., they did not converge. Addition of a steady 10-mM concentration of P_i (Fig. 5 *D*) caused the traces to converge, although not as rapidly as in the absence of Ca^{2+}. Addition of P_i also decreased the amplitude of the transient tension rise and led to more rapid decay to the steady tension level, which was lower in the presence than in the absence of P_i.

A direct comparison of traces in the presence and absence of P_i (Fig. 6) shows that 10 mM P_i did not alter the rate or amplitude of the initial tension decline after photolysis of caged ATP in the absence (*A*) or presence (*B*) of Ca^{2+}. The slow decay

portion of the in-phase stiffness signal (S) was reduced in amplitude by P_i in both the absence and presence of Ca^{2+}. The transient development of positive quadrature stiffness (Q) in the absence of Ca^{2+} and the maintained value of Q in the presence of Ca^{2+} were both reduced by including P_i in the medium.

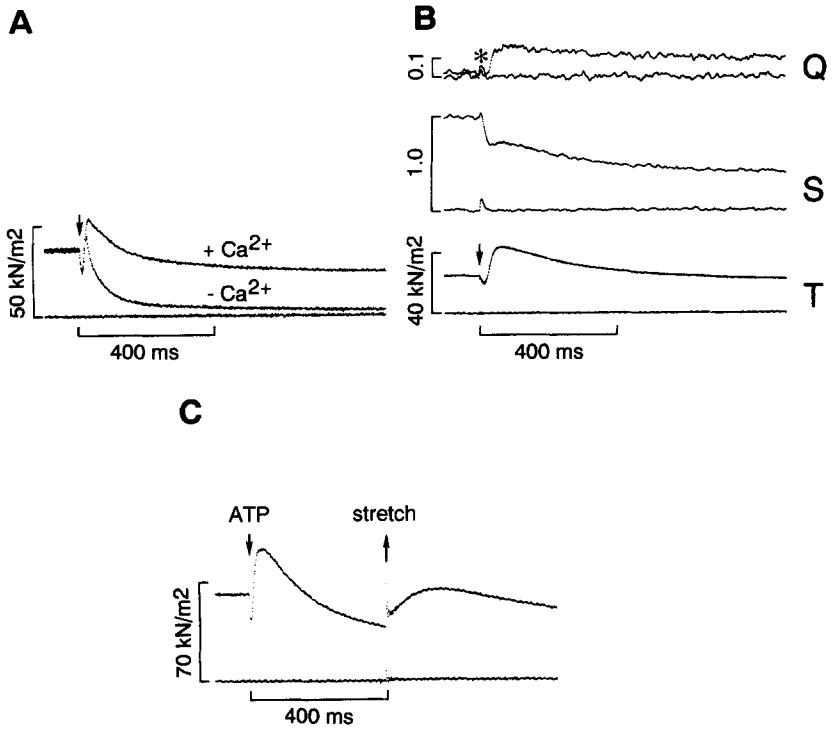

FIGURE 4. Transients initiated by caged ATP photolysis in the presence of Ca^{2+}. (*A*) Tension recordings obtained during release of 0.57 mM ATP in the absence (*middle trace*) and presence (*upper trace*) of ~30 μM free Ca^{2+}. The flat trace is a baseline recorded in relaxing solution. Fiber length, 1.24 mm; sarcomere length, 2.6 μm; cross-sectional area, 1,660 μM^2. (*B*) Tension (T), in-phase stiffness (S), and quadrature stiffness (Q) during release of 0.20 mM ATP in the presence of Ca^{2+}. The asterisk identifies an artifactual deflection caused by the laser pulse. Fiber length, 1.91 mm; sarcomere length, 2.6 μm; cross-sectional area, 3,300 μm^2. (*C*) Tension recording during release of 0.38 mM ATP (*downward arrow*) in the presence of Ca^{2+} followed by a 0.99% quick stretch (*upward arrow*) to initiate stretch activation. The lowest trace was recorded in relaxing solution during an equivalent length change. The photolysis solution had 160 mM ionic strength, 50 mM reduced glutathione, and 0 P_i. Fiber length, 1.72 mm; sarcomere length, 2.7 μm; cross-sectional area, 1,350 μm^2.

Effects of P_i on Stretch Activation

Acceleration of the approach to steady tension values in the presence of P_i and the reduction of stiffness shown in Figs. 5 and 6 are consistent with the hypothesis that P_i release from the acto-myosin-ADP-P_i complex (AM.ADP.P_i) to form a force-generat-

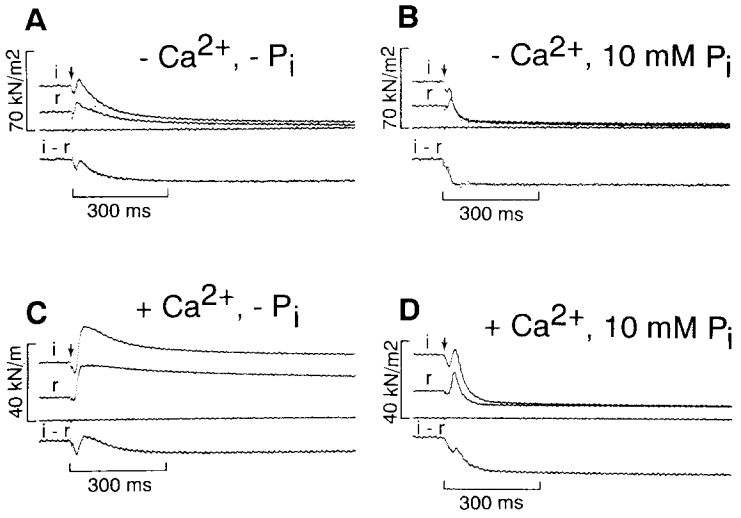

FIGURE 5. Transients initiated by photolysis of caged ATP in the absence (*A* and *C*) and presence of 10 mM P_i (*B* and *D*). Absence of Ca^{2+} (*A* and *B*); 0.29 and 0.37 mM ATP released, respectively. Isometric (*i*) and pre-release trials (*r*) using 0.5% length changes. Fiber length, 1.67 mm; sarcomere length, 3.0 μm; cross-sectional area, 1,300 μm^2. Presence of Ca^{2+} (*C* and *D*); 0.23 and 0.36 mM ATP released, respectively. Isometric (*i*) and pre-release trials (*r*) using 0.47% length changes. Fiber length, 1.76 mm; sarcomere length, 2.8 μm; cross-sectional area, 2,250 μm^2. In each panel the flat trace is a relaxed baseline and the lowest trace ($i - r$) is the numerical difference between the corresponding tension traces.

ing acto-myosin-ADP complex (AM'.ADP) is a reversible reaction step and that binding of P_i to AM'.ADP reduces cross-bridge force. This hypothesis predicts that the amplitude of stretch activation should be reduced in the presence of P_i as previously reported by White and Thorson (1972). In addition to effects of P_i on

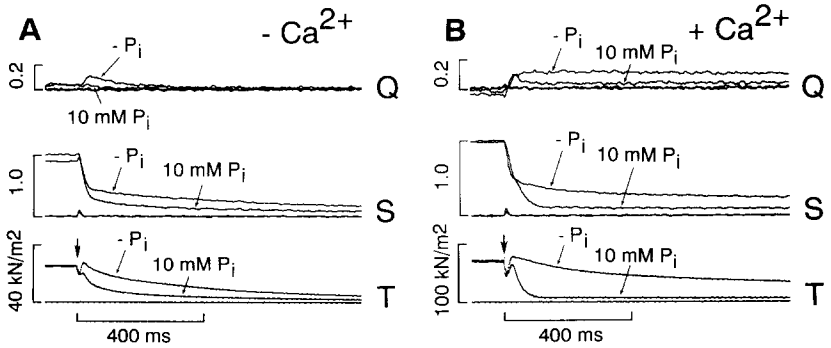

FIGURE 6. Superimposed recordings of tension (*T*), in-phase stiffness (*S*), and quadrature stiffness (*Q*) during photolysis of caged ATP in the absence and presence of 10 mM P_i. (*A*) Absence of Ca^{2+}, 0.71 mM ATP released. Fiber length, 1.69 mm; sarcomere length, 2.6 μm; cross-sectional area, 2,980 μm^2. (*B*) Presence of Ca^{2+}, 0.37 mM ATP released. Fiber length, 1.44 mm; sarcomere length, 2.6 μm; cross-sectional area, 1,350 μm^2.

tension, Fig. 7 *A* shows that 10 mM P_i also suppresses the amplitudes of the transient increase of in-phase (*S*) and quadrature (*Q*) stiffness after a quick stretch in 5 mM MgATP activating solution.

The rate of force reduction due to binding of P_i to AM'.ADP may be measured by photolysis of caged P_i during active contractions (Dantzig, Lacktis, Homsher, and Goldman, 1987; Dantzig, J. A., Y. E. Goldman, J. Lacktis, and E. Homsher, manuscript submitted for publication). In the experiment of Fig. 7, *B* and *C*, the fiber was immersed in activating solution containing 10 mM caged P_i, and at the times indicated by arrows in successive trials the P_i was released by photolysis. Trace *a* in

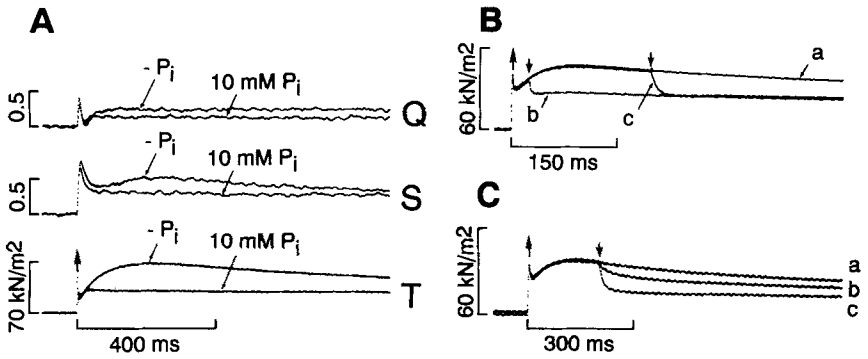

FIGURE 7. Effect of P_i on stretch activation in the presence of 5 mM MgATP and Ca^{2+}. (*A*) Superimposed recordings of tension (*T*), in-phase stiffness (*S*), and quadrature stiffness (*Q*) during stretch activation initiated by a 1.2% quick stretch in the absence (upper of each pair of traces) and presence (lower of each pair) of 10 mM P_i. The transient deflections of the *S* and *Q* traces at the time of the length change (*arrow*) and lasting ~50 ms are artifacts of the stiffness measurement technique. Fiber length, 1.42 mm; sarcomere length, 2.6 μm; cross-sectional area, 1,520 μm^2. (*B* and *C*) Photolysis of caged P_i during stretch activation. Three superimposed tension traces are shown in each panel. At the upward arrow for each trace, a quick length change was applied to the fiber to initiate stretch activation. At the downward arrows, P_i was liberated from caged P_i. In *B*, the fiber was stretched by 0.91% and 0.85 mM P_i was released for traces *b* and *c*. Fiber length, 1.36 mm; sarcomere length, 2.5 μm; cross-sectional area, 1,380 μm^2. In *C*, the fiber was stretched by 0.79% and 0.35 mM and 0.90 mM P_i was released for traces *b* and *c*, respectively. Fiber length, 1.57 mm; sarcomere length, 2.5 μm; cross-sectional area, 1,460 μm^2. The solutions for *B* and *C* had 160 mM ionic strength, 50 mM reduced glutathione, 10 mM caged P_i, and initially 0 P_i.

each case shows the tension transient during stretch activation without photolysis. In panel *B*, 850 μM P_i was released in the two photolysis trials (traces *b* and *c*). Tension decreased monotonically on photolysis of caged P_i with half-times of 3 and 6 ms for traces *b* and *c*, respectively. P_i is released from caged P_i at $\sim 2 \times 10^5\ s^{-1}$ after the laser pulse (Dantzig et al., manuscript submitted for publication), so the half-times for tension decline are not slowed by the photochemical reactions. In panel *C*, the intensity of the laser pulse was altered to release 350 μM P_i for trace *b* and 900 μM P_i for trace *c*. The amplitude of the tension decrease was graded with liberated P_i concentration. Control experiments (not shown) in which caged ATP was photolyzed during stretch activation or caged P_i was photolyzed while the fiber was in rigor

showed that the tension decreases in Fig. 7, *B* and *C*, were caused by liberation of P_i rather than the laser pulse or the by-products of photolysis.

Rate of Initial Rigor Cross-Bridge Detachment

Relaxation of tension after photolysis of caged ATP, as well as the difference between traces starting from different rigor tensions, are influenced by cross-bridges reattaching after an initial detachment by ATP. In insect muscle experiments this reattachment phase is influenced by the pre-photolysis rigor tension level, so the simple subtraction method used in rabbit muscle studies (Goldman et al., 1984*a*, *b*) could not be used to isolate the detachment step. A method was required that was independent of the tension difference traces.

The initial decrease in tension is caused by the early cross-bridge detachment and should be independent of the subsequent events if it is measured before significant cross-bridge reattachment. Therefore, the slopes of the tension traces were measured by fitting straight lines to segments of them shortly after the laser pulse. Decay of mechanical vibrations caused by the laser pulse determined the earliest time point that could be used for determining the slope. The measurement interval used was typically 4–8 ms after the laser pulse, but occasionally could begin as early as 2 ms, and at low ATP concentrations was sometimes extended to 14 ms.

To check whether the time intervals selected for measuring the initial rate of tension decay were early enough for the measured slope to be independent of cross-bridge reattachment, a simple kinetic simulation was run with rate constants similar to those estimated from the experiments. The results of this calculation using the following reaction scheme are shown in Fig. 8 *B*:

$$\text{caged ATP} \xrightarrow{k_p} \text{ATP}$$

$$\text{ATP} + \text{rigor} \xrightarrow{k_d} \text{detached} \xrightarrow{k_r} \text{active}$$

Scheme 1

where k_p = 118 s^{-1}, [caged ATP] undergoing photolysis = 1 mM, $k_d = 2 \times 10^5$ $M^{-1}s^{-1}$, and k_r = 30 s^{-1} for the upper trace in Fig. 8 *B* and k_r = 0 for the lower trace. The two traces follow a similar time course for ~10 ms, indicating that for these values of the rate constants, the initial slope reflects mainly detachment rate (k_d). Straight lines fitted in the 3–7-ms interval of the two simulated traces of Fig. 8 *B* intercept the zero tension level at times differing by 11%, indicating an 11% bias in estimating k_d from the intercept time. The error increases to 15% if the regression interval is 3–20 ms.

Fig. 8 *A* shows the lines fitted to two tension traces that started at different rigor tensions. The lines intersected the relaxed baseline at approximately the same time (t_i), indicating that the slopes were directly proportional to the initial rigor tension, and the rate constant for detachment does not depend on the level of rigor tension.

Apparent rate constants for cross-bridge detachment in a series of experiments were calculated as the reciprocal of the time between the laser pulse and the intersection of the fitted straight line with the relaxed force baseline ($k_{obs} = 1/t_i$). This method of analysis is based on the assumption that tension in an attached cross-bridge is eliminated when it detaches. The k_{obs} values are plotted in Fig. 9 against the

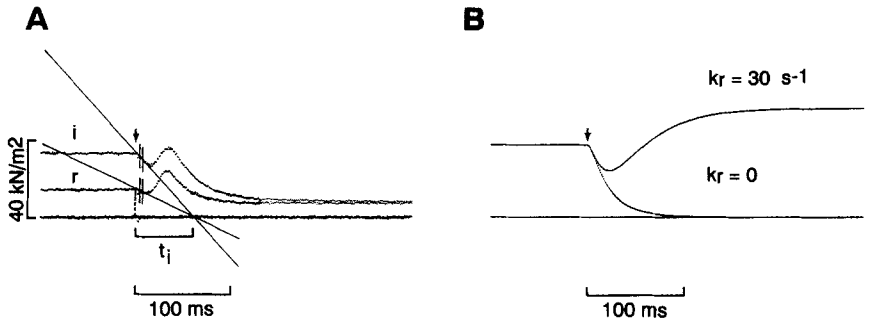

FIGURE 8. Method of extracting the initial detachment rate from tension traces recorded in photolysis trials. (*A*) Isometric (*i*) and pre-release (*r*, 0.47%) conditions when 0.36 mM ATP was released from caged ATP in the presence of 30 μM free Ca^{2+} and 10 mM P_i. The straight lines are fit by linear regression to the tension data in the interval (between the two vertical bars) 3–6 ms after the laser pulse. The characteristic time, t_i, for the fitted line to intersect the relaxed tension level is related to the rate of cross-bridge detachment. Fiber length, 1.76 mm; sarcomere length, 2.8 μm; cross-sectional area, 2,250 μm^2. (*B*) Computer simulations to estimate the effect of reattachment and tension development on the initial slope of the tension decline. The reaction scheme and rate constants are described in the text. The upper trace includes simulated reattachment; the lower trace simulates pure detachment by ATP. The two traces separate at ~7 ms after the simulated laser pulse.

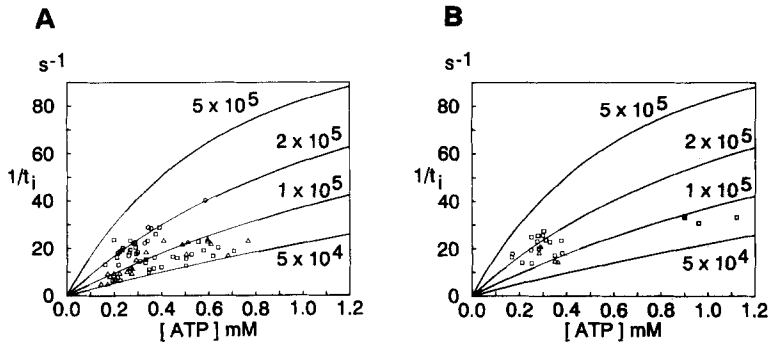

FIGURE 9. ATP dependence of detachment rates for rigor cross-bridges in the absence (*A*) and presence (*B*) of Ca^{2+}. The apparent detachment rates ($1/t_i$), determined as shown in Fig. 8, were plotted vs. liberated ATP concentrations determined by HPLC. Data represented by squares were obtained in the absence of P_i (n = 61, 24 fibers), and those represented by triangles were obtained in the presence of 10 mM P_i (n = 26, 10 fibers). Circles in *A* were obtained in the absence of Ca^{2+} and P_i from freshly dissected and mechanically skinned single fibers (n = 5, three fibers). The curves represent rates expected from reaction Scheme 1 of the text, including the 118 s^{-1} photochemical dark reaction preceding ATP release. A series of traces were simulated using liberated ATP concentrations between 50 μM and 1.2 mM and second order rate constants for ATP-induced cross-bridge detachment from 5×10^4 to 5×10^5 $M^{-1}s^{-1}$. These simulated traces were fitted with straight lines (as in Fig. 8 *A*) and the apparent detachment rates ($1/t_i$) were plotted as in the case of the experimental data. Smooth curves were drawn through the simulated data points using cubic spline interpolation.

released concentration of ATP. *A* shows data from a total of 68 photolysis trials (26 fibers) in the absence of Ca^{2+}. Isometric, pre-stretch, and pre-release protocols in the absence of P_i are shown as squares. No consistent effect of initial rigor tension on detachment rate was noted. Data from experiments conducted at 10 mM P_i are plotted as triangles. The circles represent data (at 0 P_i) from freshly dissected, mechanically skinned fibers, which did not undergo glycerol extraction and freezer storage.

The curves in Fig. 9 were calculated from Scheme 1 above using $k_r = 0$ and $k_d = 5 \times 10^4$–5×10^5 $M^{-1}s^{-1}$ as indicated next to each curve. Straight lines were fitted to the simulated traces in the 3–7-ms interval and $1/t_i$ was plotted vs. the concentration of released ATP in the simulation as for the experimental data. This procedure corrects for the dark reaction time of ATP release from caged ATP and the limited ATP and myosin head concentrations (Goldman et al., 1984*a*).

Fiber to fiber variation is considerable, but there is a trend toward higher observed detachment rates at the higher ATP concentrations. Although the points from the mechanically skinned fibers are near the top range of the data, most of the points fall in the range expected for $k_d = 5 \times 10^4$–2×10^5 $M^{-1}s^{-1}$. The measured detachment rates are similar in the absence and presence of P_i (see also Fig. 6).

Fig. 9 *B* indicates the equivalent plot of $1/t_i$ vs. ATP concentration from a total of 24 trials (8 fibers) in the presence of Ca^{2+}. Squares represent data at 0 P_i and triangles represent data at 10 mM P_i. Most of the data points fall between the curves for $k_d = 5 \times 10^4$ and 2×10^5 $M^{-1}s^{-1}$. Comparison of Fig. 9 *A* and *B* suggests that Ca^{2+} does not affect detachment rate (see also Fig. 4 *A*).

DISCUSSION

Mechanical tension and stiffness transients after laser photolysis of caged ATP in insect asynchronous muscle had many qualitative characteristics similar to those reported previously for vertebrate (rabbit) skeletal muscle (Goldman et al., 1984*a*, *b*), indicating rapid detachment of rigor cross-bridges by ATP and cooperative reattachment and force generation even in the absence of Ca^{2+} in both systems. In the absence of Ca^{2+} and P_i, tension traces starting from different rigor force levels maintained the tension difference until relaxation was complete (Figs. 1 *B*, 3, *A* and *B*, and 5 *A*), in contrast to the behavior of rabbit fibers in which the traces converge to a common time course well before final relaxation (Fig. 3 *C*). Addition of P_i to the medium accelerated the convergence (Fig. 5 *B*). These results suggest that when a stretch is applied to the fiber, the likelihood of cross-bridge attachment into force-generating states is enhanced.

Events during ATP-induced Relaxation

When 0.1–1 mM ATP was released into the insect fiber filament lattice in the absence of Ca^{2+}, relaxation of tension and stiffness proceeded in several phases. (1) An initial rapid decrease in tension and stiffness, indicating detachment of rigor cross-bridges, was followed by (2) a transient phase of active tension redevelopment due to reattaching cross-bridges, and then (3) a slower decrease to the relaxed baseline, indicating final detachment. Several observations provide support for this interpreta-

tion of the transients. The first tension decrease (phase 1) after ATP liberation is faster and more prominent when ATP concentration is increased (Fig. 2 *C*), but is insensitive to Ca^{2+} (Fig. 4 *A*) or P_i (Fig. 6). Tension development during phase 2 is accompanied by decreasing in-phase stiffness (Fig. 2 *A*, trace *S*, related to the number of attached cross-bridges) and a positive deflection of the quadrature stiffness (Fig. 2 *A*, trace *Q*, indicating cross-bridge viscoelasticity). Thus the cross-bridges present at the peak of the tension rise have the high force and quick stress relaxation of actively force-generating attachments. Increasing the concentration of ATP (Fig. 2 *C*) or including 10 mM P_i in the photolysis medium (Figs. 5 and 6) markedly decreased the amplitude of the transient tension rise and accelerated final relaxation.

These results are consistent with force generation during phase 2 of cross-bridges that reattach because the Ca^{2+} regulatory system is switched on by remaining nucleotide-free cross-bridges (rigor links). Then the amplitude of the transient tension rise is reduced at high ATP concentration because the likelihood of reattachment before elimination of neighboring rigor links is decreased as [ATP] is increased. The force and lifetime of a reattachment would be decreased in the presence of P_i if P_i binds to the active site on force-generating AM.ADP complexes to generate the low force, quickly detaching AM.ADP.P_i state.

Other possible explanations should be considered for the transient increase of tension observed after release of ATP into the filament lattice. AM.ATP complexes might generate more force than rigor (AM) complexes. In this case, the tension rise would be expected to increase in amplitude with ATP concentration, whereas the amplitude decreased (Fig. 2 *C*). Also, the observed fall in stiffness during the tension increase (Fig. 2 *A*) would not be expected. Another possibility is that some of the rigor cross-bridges are under negative strain before the laser pulse. If that group of cross-bridges detached more rapidly than the cross-bridges under normal positive strain, tension would increase. If that mechanism were a prominent factor, the time course of the transients would have depended strongly on the initial rigor tension level, which was not observed. Also, the positive deflection of the quadrature trace would not be expected. Although some contribution from high force AM.ATP cross-bridges and from rapid detachment of negatively strained cross-bridges cannot be excluded, the data are most consistent with the tension rise being due to reattaching cross-bridges that develop active force.

Rate of ATP-induced Detachment of Rigor Cross-Bridges

The initial tension decay increased in rate and amplitude with ATP concentration (Figs. 2 *C* and 9) and was not sensitive to P_i concentration (Figs. 6 and 9). These characteristics suggest that it represents the detachment of rigor cross-bridges by photochemically liberated ATP. The subsequent reattachment phase complicates quantitative analysis, but the slope of the early tension decline (Fig. 8 *A*) provides an estimate of the detachment rate with little contamination from the subsequent processes. The slope of the early tension decline was proportional to the starting rigor tension (Fig. 8 *A*), which is consistent with little, if any, influence of filament stress or strain on the detachment rate of AM by ATP.

ATP detaches rigor cross-bridges with a second order rate constant in the range 5×10^4–2×10^5 $M^{-1}s^{-1}$. These values are within an order of magnitude of the rate

constant for ATP-induced dissociation of acto-myosin subfragment-1, measured in solution for insect myosin (White, Zimmerman, and Trentham, 1986). Thus assembly of the proteins into the filament lattice does not markedly alter the rate of this reaction. At physiological ATP concentration (~5 mM), the expected rate for cross-bridge detachment from the AM state is at least 250 s^{-1} (5×10^4 $M^{-1}s^{-1} \times 5$ mM). This rate is much faster than the 1.4–3 s^{-1} rate of ATP hydrolysis per myosin head (Lund, Webb, and White, 1988), leading to the conclusion that ATP-induced detachment is too fast to contribute to rate limitation of cross-bridge cycling. Since ATP-induced detachment is not sensitive to Ca^{2+} (Figs. 4 *A* and 9), this reaction does not seem to be a physiological control point. The rate-limiting step in the fully activated cross-bridge cycle is presumably earlier in the sequence of transitions between attached states (White, Lund, and Webb, 1988). These interpretations and conclusions are all similar to those discussed in more detail for rabbit muscle by Goldman et al. (1984*a*, *b*).

X-ray diffraction experiments on insect muscle during photolysis of caged ATP (Poole, Rapp, Maéda, and Goody, 1988) are consistent with these conclusions except that the second order rate constant estimated from the kinetics of the equatorial reflection changes was even higher (~10^6 $M^{-1}s^{-1}$) than the values reported here. Marcussen and Kawai (1990) also obtained nearly ~10^6 $M^{-1}s^{-1}$ for the detachment rate using sinusoidal analysis. The detachment rate constant obtained in the present study may be lowered partly by binding of caged ATP to the rigor cross-bridges and partly by some reattachment during the interval used for determining the slope of the initial tension decline.

A surprising finding in the x-ray diffraction results was that the ratio of equatorial reflections reached the relaxed value and was stable well before final tension relaxation. Our data (e.g., Figs. 2 *A* and 6 *A*) indicate that, on average, the slow phase of tension relaxation corresponds to 35% of the total stiffness decline. In rabbit fibers the corresponding value for the proportion of stiffness decline in the slow phase is higher (~50%). A slow final phase of the change in x-ray equatorial ratio has been observed during relaxation of rabbit fibers after photolysis of caged ATP (Poole et al., 1988). It appears that force-generating cross-bridges, attached during the later phases of the transients, are not detected in the equatorial x-ray reflections in insect fibers.

Effects of P_i

P_i decreases the amplitude of stretch activation (Fig. 7 *A*) as has been previously reported (White and Thorson, 1972), and photolysis of caged P_i during stretch activation caused a rapid fall of tension (Fig. 7 *B*). These results are consistent with the hypothesis that P_i in the medium can bind to a force-generating AM.ADP intermediate to form AM.ADP.P_i, which supports less force. This hypothesis was proposed on the basis of caged ATP photolysis experiments in rabbit fibers (Hibberd et al., 1985) and has received support from oxygen exchange studies showing that P_i does bind to the active site of AM.ADP in rabbit (Webb, Hibberd, Goldman, and Trentham, 1986) and insect (Lund et al., 1988) muscle fibers. The rate of P_i release, detected in the oxygen exchange studies, is slower in insect fibers (Lund et al., 1988). If P_i release is concomitant with tension development during stretch activation, then

as tension rises, population of the AM.'ADP state would increase. This momentary redistribution of the biochemical states might explain the increased amplitude of the tension drop when caged P_i was photolyzed late in stretch activation compared with that obtained on photolysis just after the mechanical stretch (Fig. 7 *B*).

Inclusion of a steady 10-mM concentration of P_i in the caged ATP photolysis medium markedly accelerated the final phase of tension and stiffness relaxation (Figs. 5 and 6), as expected if P_i release is reversible and AM.'ADP bears more force than AM.ADP.P_i. The final relaxation is then partly via the route AM.'ADP → AM.ADP.P_i → M.ADP.P_i (i.e., by reversal of cross-bridge attachment). These results suggest that the structural change leading to the force-generating state is linked to P_i release from AM.ADP.P_i.

Nonconvergence of Tension Traces

A conspicuous difference between the results on insect flight muscle presented here and the corresponding experiments with rabbit psoas fibers was that tension recordings in insect fibers starting from different rigor levels did not converge before final relaxation unless inorganic phosphate was present in the medium (Figs. 1 *B*, 3, *A* and *B*, and 5, *A* and *B*). With rabbit fibers, when pre-stretches or pre-releases were applied 1 s before the laser pulse, the traces starting from different rigor tensions converged approximately at the peak of the transient tension rise whether or not P_i was added to the photolysis medium (Goldman et al., 1984*a*; Hibberd et al., 1985; Fig. 3 *C* of this article). The convergence has been interpreted as indicating detachment of all the original rigor cross-bridges with concomitant loss of the strain increment imposed by the pre-photolysis length change. Nonconvergence in the insect fiber experiment thus implies either (*a*) incomplete detachment of rigor cross-bridges at the peak of the tension rise or (*b*) retention of some aspect of pre-photolysis strain even after cross-bridge detachment.

Of these two hypotheses, several of our results make (*b*) more plausible. The slow component of the tension difference trace (Figs. 3, *A* and *B* and 5 *A*) was noticeably reduced or abolished when 10 mM P_i was included in the medium, suggesting that slow convergence of the tension traces is due to reattachments instead of incomplete detachment. When Ca^{2+} was present in the photolysis medium, the transients were similar to those in the absence of Ca^{2+} except that the transient tension rise was greater in magnitude and there was partial maintenance of steady tension and stiffness (Figs. 4 and 5). In the medium containing Ca^{2+}, tension traces converged slowly or not at all unless P_i was present (Fig. 5), further supporting the hypothesis that the slowly decaying component of the tension difference trace is due to reattaching cross-bridges.

Following ATP release after a pre-stretch, the increased amplitude of transient force development could be caused either by enhanced force per cross-bridge or increased numbers of attached cross-bridges. Cross-bridge attachment could be increased either by changes in the attachment/detachment rate constants or by a change in the number of cross-bridges capable of attaching. Pre-photolysis length changes caused very little change of timing among the various phases of the transients (Figs. 1 *B*, 3, *A* and *B*, 5, and 8 *A*), even though peak tension often differed by a factor of two or more. This argues against a change in the attachment or detachment rate constants, and thus supports the hypothesis that the pre-photolysis

length changes modulate the number of cross-bridges capable of entering the cross-bridge cycle.

Structural analysis of the filament periodicities and orientations led Wray (1979) to propose that length changes would alter the number of myosin projections apposed to thin filament "target zones" with the appropriate orientation for attachment. The increased number of potential attachments after a stretch could lead to enhanced tension development after caged ATP photolysis. Since we observed increased tension without a substantial change in the kinetics, our results support the idea that the stretch increases the number of myosin heads aligned with thin filament target zones.

Relevance to Stretch Activation

The tension rise after caged ATP photolysis is similar in some respects to stretch activation. Both processes are enhanced by stretch. High tension per unit stiffness indicates high force per attachment in both cases. A positive deflection of the quadrature stiffness accompanies tension development after both stretch activation and photolysis (Fig. 2, *A* and *B*). Both processes are suppressed by P_i.

But some significant differences exist in the two types of transient tension development. In-phase stiffness increases during stretch activation and decreases after photolysis. At comparable ATP concentrations, the time course of the tension rise is more rapid after caged ATP photolysis from rigor than after a quick stretch in activating solution (Figs. 1, 2, and 4 *C*). Since the length changes in photolysis experiments were applied 0.5 or 1 s before the laser pulse, any rate processes associated with the switching mechanism of stretch activation would be complete by the time of the laser pulse. The faster tension development after photolysis thus suggests that a rate process related to the switching mechanism rather than cross-bridge attachment itself limits the kinetics of stretch activation. Simple recruitment of cross-bridges by increased alignment between myosin heads and target zones would not meet this condition. Many other studies have documented changes in rate constants within the cross-bridge cycle during stretch activation (Thorson and White, 1969, 1983; Güth et al., 1987; Lund et al., 1988).

A puzzling aspect of our results is that the tension and stiffness transients after photolysis were reproducible even when stretch activation was suppressed after several photolysis trials. This result suggests that the length-sensing or switching mechanism rather than the cross-bridge cycle itself is modified by the experimental procedure. It is not certain whether the length-sensing mechanism for enhanced tension development after photolysis is the same as for stretch activation. In fact, we do not have evidence that the filaments actually slide when the length changes are applied to rigor insect fibers (Reedy, M. K., personal communication). But on detachment after release of ATP the filaments presumably accommodate to the length changes by sliding motions and then the pre-stretch is expressed as enhanced tension development.

Conclusions

ATP rapidly detaches nucleotide-free (rigor) cross-bridges in asynchronous insect flight muscle. This step does not seem to limit or control the rate of cross-bridge cycling. Length changes in rigor modulate the force due to cross-bridges reattaching

after ATP-induced detachment. The results support the hypothesis that alignment between matching periodicities of the thick and thin filaments in insect flight muscle modulates transient tension development after caged ATP photolysis. The same mechanism may be involved in stretch activation, but additionally, control of rate constants within the cross-bridge cycle by a stress or strain sensor seems to be required.

We thank Dr. D. C. S. White for helpful discussion of the manuscript.

This work was supported by a post-doctoral fellowship (to M. Yamakawa), a research grant from the Muscular Dystrophy Associations of America, and NIH grant AR-26846.

REFERENCES

Abbott, R. H., and P. E. Cage. 1984. A possible mechanism of length activation in insect fibrillar flight muscle. *Journal of Muscle Research and Cell Motility.* 5:387–397.

Ashhurst, D. E. 1967. The fibrillar flight muscles of giant water-bugs: an electron-microscope study. *Journal of Cell Science.* 2:435–444.

Auber, J., and R. Couteaux. 1963. Ultrastructure de la strie Z dans des muscles de diptères. *Journal de Microscopie.* 2:309–324.

Bozler, E. 1972. Feedback in the contractile mechanism of the frog heart. *Journal of General Physiology.* 60:239–247.

Bullard, B., K. Leonard, A. Larkins, G. Butcher, C. Karlik, and E. Fyrberg. 1988. Troponin of asynchronous flight muscle. *Journal of Molecular Biology.* 204:621–637.

Dantzig, J. A., J. W. Lacktis, E. Homsher, and Y. E. Goldman. 1987. Mechanical transients initiated by photolysis of caged P_i during active skeletal muscle contractions. *Biophysical Journal.* 51:3*a*. (Abstr.)

Goldman, Y. E., M. G. Hibberd, J. A. McCray, and D. R. Trentham. 1982. Relaxation of muscle fibres by photolysis of caged ATP. *Nature.* 300:701–705.

Goldman, Y. E., M. G. Hibberd, and D. R. Trentham. 1984*a*. Relaxation of rabbit psoas muscle fibres from rigor by photochemical generation of adenosine-5′-triphosphate. *Journal of Physiology.* 354:577–604.

Goldman, Y. E., M. G. Hibberd, and D. R. Trentham. 1984*b*. Initiation of active contraction by photogeneration of adenosine-5′-triphosphate in rabbit psoas muscle fibres. *Journal of Physiology.* 354:605–624.

Goldman, Y. E., and R. M. Simmons. 1984. Control of sarcomere length in skinned muscle fibres of *Rana temporaria* during mechanical transients. *Journal of Physiology.* 350:497–518.

Güth, K., K. J. V. Poole, D. Maughan, and H. J. Kuhn. 1987. The apparent rates of crossbridge attachment and detachment estimated from ATPase activity in insect flight muscle. *Biophysical Journal.* 52:1039–1045.

Hibberd, M. G., J. A. Dantzig, D. R. Trentham, and Y. E. Goldman. 1985. Phosphate release and force generation in skeletal muscle fibers. *Science.* 228:1317–1319.

Jewell, B. R., and J. C. Rüegg. 1966. Oscillatory contraction of insect fibrillar muscle after glycerol extraction. *Proceedings of the Royal Society of London, Series B.* 164:428–459.

Kaplan, J. H., B. Forbush III, and J. F. Hoffman. 1978. Rapid photolytic release of adenosine 5′-triphosphate from a protected analogue: Utilization by the Na:K pump of human red blood cell ghosts. *Biochemistry.* 17:1929–1935.

Lund, J., M. R. Webb, and D. C. S. White. 1988. Changes in the ATPase activity of insect fibrillar flight muscle during sinusoidal length oscillation probed by phosphate-water oxygen exchange. *Journal of Biological Chemistry.* 263:5505–5511.

Marcussen, B. L., and M. Kawai. 1990. Role of MgATP and inorganic phosphate ions in cross-bridge kinetics in insect (*Lethocerus colossicus*) flight muscle. *In* Frontiers in Smooth Muscle Research. N. Sperelakis and J. D. Wood, editors. Alan R. Liss, Inc., New York. 805–813.

McCalla, T. R. 1967. Introduction to Numerical Methods and FORTRAN Programming. John Wiley & Sons, Inc., New York. 359 pp.

Nave, R., and K. Weber. 1990. A myofibrillar protein of insect muscle related to vertebrate titin connects Z band and A band: purification and molecular characterization of invertebrate mini-titin. *Journal of Cell Science.* 95:535–544.

Poole, K. J. V., G. Rapp, Y. Maéda, and R. S. Goody. 1988. The time course of changes in the equatorial diffraction patterns from different muscle types on photolysis of caged-ATP. *Advances in Experimental Medicine and Biology.* 226:391–401.

Pringle, J. W. S. 1978. The Croonian Lecture, 1977. Stretch activation of muscle: function and mechanism. *Proceedings of the Royal Society of London, Series B.* 201:107–130.

Reedy, M. K., K. C. Holmes, and R. T. Tregear. 1965. Induced changes in orientation of the cross-bridges of glycerinated insect flight muscle. *Nature.* 207:1276–1280.

Steiger, G. J. 1971. Stretch activation and myogenic oscillation of isolated contractile structures of heart muscle. *Pflügers Archiv.* 330:347–361.

Taylor, K. A., M. C. Reedy, L. Córdova, and M. K. Reedy. 1989. Three-dimensional image reconstruction of insect flight muscle. II. The rigor actin layer. *Journal of Cell Biology.* 109:1103–1123.

Thorson, J., and D. C. S. White. 1969. Distributed representations for actin-myosin interaction in the oscillatory contraction of muscle. *Biophysical Journal.* 9:360–390.

Thorson, J., and D. C. S. White. 1983. Role of cross-bridge distortion in the small-signal mechanical dynamics of insect and rabbit striated muscle. *Journal of Physiology.* 343:59–84.

Walker, J. W., G. P. Reid, J. A. McCray, and D. R. Trentham. 1988. Photolabile 1-(2-nitrophenyl)ethyl phosphate esters of adenine nucleotide analogues. Synthesis and mechanism of photolysis. *Journal of the American Chemical Society.* 110:7170–7177.

Webb, M. R., M. G. Hibberd, Y. E. Goldman, and D. R. Trentham. 1986. Oxygen exchange between P_i in the medium and water during ATP hydrolysis mediated by skinned fibers from rabbit skeletal muscle. *Journal of Biological Chemistry.* 261:15557–15564.

White, D. C. S. 1983. The elasticity of relaxed insect fibrillar flight muscle. *Journal of Physiology.* 343:31–57.

White, D. C. S., J. Lund, and M. R. Webb. 1988. Cross-bridge kinetics in asynchronous insect flight muscle. *Advances in Experimental Medicine and Biology.* 226:169–178.

White, D. C. S., and J. Thorson. 1972. Phosphate starvation and the nonlinear dynamics of insect fibrillar flight muscle. *Journal of General Physiology.* 60:307–336.

White, D. C. S., and J. Thorson. 1973. The kinetics of muscle contraction. *Progress in Biophysics and Molecular Biology.* 27:173–255.

White, D. C. S., R. W. Zimmerman, and D. R. Trentham. 1986. The ATPase kinetics of insect fibrillar flight muscle myosin subfragment-1. *Journal of Muscle Research and Cell Motility.* 7:179–192.

Wray, J. S. 1979. Filament geometry and the activation of insect flight muscles. *Nature.* 280:325–326.

Yamakawa, M., K. Güth, M. G. Hibberd, and Y. E. Goldman. 1985. Relaxation of insect asynchronous flight muscle by photolysis of caged ATP. *Biophysical Journal.* 47:288*a*. (Abstr.)